*International Journal of Research in Advent Technology, Special Issue, March 2019*
*E-ISSN: 2321-9637*
*3rd National Conference on Recent Trends & Innovations In Mechanical Engineering*
*15th & 16th March 2019*
*Available online at* www.ijrat.org

# Flow Simulation Analysis Of Horizontal Wind Turbine Rotor Blade

[1] Lakshmigalla Sunil Kumar, [2]CH Soundarya , [3]Telkar Mahesh, [4]Jagilam Kumar Chandra
[1] *Assistant Professor,* [2] *PG Scholar,* [3]*Assistant professor,* [4]*Assistant professor*
*Department of ME, NNRG, Hyderabad*

**Abstract**
A wind turbine is a rotary device that extracts energy from the wind. Wind energy has been shown to be one of the most viable sources of renewable energy. With current technology, the low cost of wind energy is competitive with more conventional sources of energy such as coal. Rotor blade is a key element in a wind turbine generator system to convert wind energy in to mechanical energy. Most blades available for commercial grade wind turbines incorporate airfoil shaped cross sections. These blades are found to be very efficient at lower wind speeds in comparison to the potential energy that can be extracted. In this project, static and flow simulation of wind turbine rotor blade for aero foilMH 102 type. In this we design three types of designs by changing bend angles and show which is best, based on the results. For the design of blades and flow analysis Solid works 2014 software is used and for static analysis Ansys 16.0 is used.
**Keywords —** Airfoil MH 102, Von-mises stress, total deformation, Solid Works 2014 and Ansys 16.0.

## 1. INTRODUCTION

### *1.1 Wind Turbine:*

A wind turbine is a device that converts the wind's kinetic energy into electrical energy.

Wind turbines are manufactured in a wide range of vertical and horizontal axis.

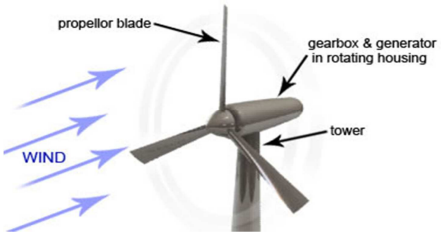

Fig.1: Wind turbine

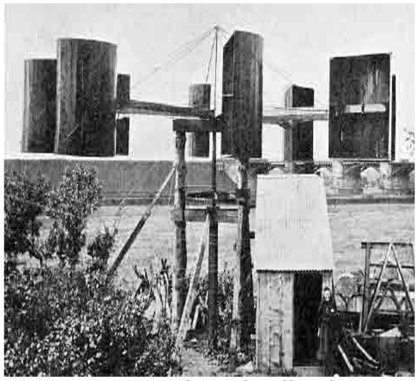
Fig.2: First vertical wind mill turbine


Fig.3:First horizontal wind mill turbine

## 2. WORKING PRINCIPLE:

Wind turbines operate on a simple principle. The energy in the wind turns two or three propeller-like blades around a rotor. The rotor is connected to the main shaft, which spins a generator to create electricity.

A wind turbine works the opposite of a fan. Instead of using electricity to make wind, like a fan, wind turbines use wind to make electricity. The wind turns the blades, which spin a shaft, which connects to a generator and makes electricity.

*International Journal of Research in Advent Technology, Special Issue, March 2019*
*E-ISSN: 2321-9637*
*3rd National Conference on Recent Trends & Innovations In Mechanical Engineering*
*15th & 16th March 2019*
*Available online at* www.ijrat.org

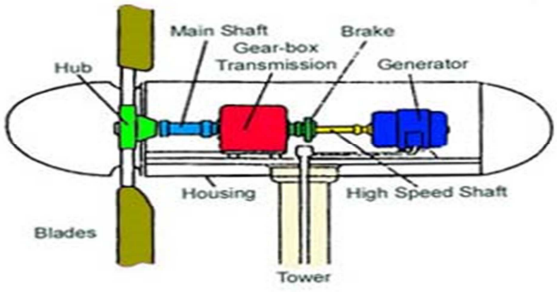


Fig.4: Working of wind turbine

***1.2 Wind-Turbine Blade Material Selection:***

From simple consideration of basic functional and longevity requirements for a HAWT blade it can be readily concluded that the main blade material-selection indices must be based on the following material properties:

(a) A high material stiffness to ensure retention of the optimal aero-dynamic shape by the blade while subjected to strong-wind loading conditions;
(b) A low mass density to minimize gravity-based loading;
(c) A large, high-cycle fatigue strength to ensure the required 20-year life cycle with high reliability.

As mentioned earlier, the HAWT-blade is essentially a cantilever beam. If the materials election methodology proposed by Ash by is utilized, then the first material selection index can be defined by requiring that the blade attains a minimal mass while meeting the specified bending-stiffness requirements (or alternatively that the blade attains maximum bending stiffness at a given mass level). Since the blade mass scales directly with its average cross-sectional area while its, stiffness scales roughly with the square of its, cross-sectional area, following Ashby's material selection procedure one can readily derive the following "*light, stiff beam*" material selection index:

$$M_1 = E^{1/2} / \rho$$

Where $E$ is the material's Young's modulus and $\rho$is its density.

The use of 1 $M$ in the HAWT-blade material selection would normally identify foam-like materials as potential candidates. In these materials, their low stiffness (as quantified by the value of their Young's modulus, $E$) is more than compensated by their low □ value. Consequently, $M$ takes on a large value in the case of foam materials suggesting their suitability for use in the HAWT-blade applications. However, foam materials would yield very bulky blades which could present serious design, manufacturing, installation and operational problems. In addition, potentially open-cell structure and the associated high water-permeability/moisture-absorption can disqualify these materials from being used in the HAWT-blade applications. To overcome these problems, a second material selection index (more precisely, a lower-bound material property limit) is proposed which requires that the HAWT-blade materials possess a minimal level of absolute stiffness, i.e.

$$M_2 \geq E$$

Typically, the minimal level of the Young's modulus required for a given-blade material is in a 15-20GPa range.

The two material selection indices defined above utilize two ($E$ and $\rho$) out of the three previously identified material properties. Inclusion of the third material property (the fatigue strength) into a material selection index is, however, quite challenging. The reason is that, as discussed in the previous section, while the constant-amplitude fatigue strength associated with a given load mean-value and a given fatigue life can be readily determined HAWT-blade material selection requires the use of a variable-amplitude fatigue life.

## 3. OBJECTIVE OF THE STUDY:

- In this project, static and flow simulation of Horizontal wind turbine rotor blade for aero foil MH 102 type.
- In this we design three types of designs by changing bend angles and show which is best, based on the results.
- For the design of blades and flow analysis Solid works 2014 software is used and for static analysis Ansys 16.0 is used.

## 4. LITERATURE REVIEW

Over the years, wind turbine blades has gone through many phases of development, researchers are still trying to improve the performance of the wind turbine. In this section a review is carried out on work done by various researches in the area of performance improvement of the wind turbine blade and its optimization.

Saxena and Agrawal [1] analyzed a basic aerodynamic theory of wings and the provided and methodology for wind tunnel testing. They found angle of attack at which the lift is maximized in order to get the best performance of this wing when in flight.

McCosker [2] designed a wind turbine using NACA 4412 profile for residential use.

Óskarsdóttir [3] gives a general account and evaluation of (HAWT) horizontal axis wind turbines and (VAWT) vertical axis wind turbines.Baldacchino [4] determined the existence of the earth and exterior distresses, most particularly, alterations in wake pitch and the rotor thrust coefficient. Sherry et. al [5] studied the vortex interface and steadiness of the helical whirlpool strands within a (HAWT) horizontal axis wind turbine wake. Serhat Duran [6] studied

HAWT blade design from the aspect of aerodynamic view and the basic principles of the aerodynamic behaviors of HAWTs. DeCoste et al. [7] designed a vertical axis wind turbine using NACA 0012 aero foil structure. MATLAB software is used to obtain lift and drag coefficients, angles of attack and relative wind speeds. Herbert et al. [8] discussed the design procedure and outcomes of the sandia 34.1-m VAWT Test Bed platform and the FloWind prototype development platform with a sense toward future offshore designs.Castillo [9] designed a small (VAWT) vertical axis wind turbine rotor with the hard timber as a building material. The smooth analysis was performed employing a thrust based model on a scientific main frame program. Deisadzeet al. [10] studied the potential for installing roof-mounted vertical axis wind turbine (VAWT) systems on house roofs. Yu-MIng et al [11] performed analysis based on structure first approach which proposed the constraint expressions of blade which have fine structure. Narimahet al. [12] carried out analysis using Autodesk Inventor to develop three dimensional model of NACA 4412 airfoil blades with and without slot before assessment of smooth features by using ANSYS software. Manyonge et al. [13] made a mathematical model of wind turbine to understand the behaviour of the wind turbine over its region of operation. According to Bergey [14], Griffiths, the maximum conversion efficiency of the horizontal axis wind turbine (HAWT) is 16/27. Air is treated stationery, non-viscous and incompressible in the flow analysis. Unique main significance of wind turbine design is its number of blades. Number of blades is significantly prompting, the horizontal axis wind turbines (HAWT). Most common number used are 2 and 3 blades. Nearly some HAWTs might have more than 3 blades, and usually because they are used for low speed wind turbines and most of the current viable turbines used for power generation have three blades. It is well-known that additional blades offer a larger available surface area for the wind to push, so it would yield additional rotating power but in the similar period a larger number of blades upsurge the weight to be rotated by the turbine. Bottasso [15] described a method for the structural optimization of wind turbine rotor blades for given prescribed aerodynamic shape. The study of Snel [16] gives overview of different methods, to evaluate the aerodynamic performance of wind turbine. Hosman made a performance analysis and improvement of small wind turbine. Aboutanalyzed the properties of airfoil using 32 theory of airfoil section. According to Grifith, the output power of the turbine depends on lift/drag ratio. Hassanien et al.[17] stated that the selection of airfoil should be so that location along the blade ensures highest contribution to the overall performance. Sepera studied the Wilson's methods of blade design. The main objective of the revision is to improve the power coefficient of wind turbine using appropriate blade design at rated wind speed. Maalawi et al. studied the theoretical optimum distribution of the inflow angle using trigonometric function methods which are based on ideal condition. Thumthae and Chitsomboon presented the arithmetical simulation of (HAWT) horizontal axis wind turbines with uncoiled edge in the steady state condition. The objective was to investigate the situation for the optimum pitch that yields the maximum power production.

***Solid Works***

Solid Works is mechanical design automation software that takes advantage of the familiar Microsoft Windows graphical user interface.

It is an easy-to-learn tool which makes it possible for mechanical designers to quickly sketch ideas, experiment with features and dimensions, and produce models and detailed drawings.

***Modeling Of Blade:***

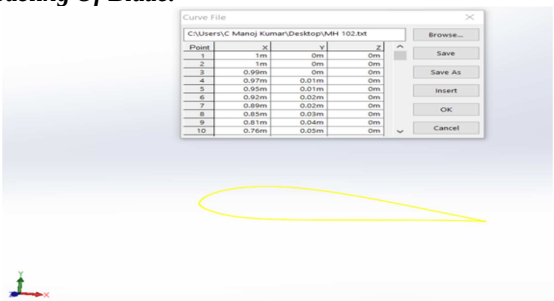


Fig.6: After opening the solid works software, import the curve points and click ok

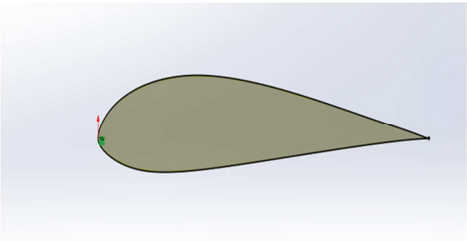

Fig.7: sketch and click convert entities then select curve and it is formed a sketch.

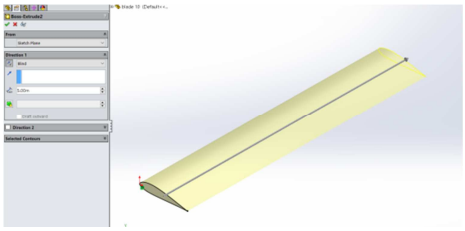

Fig.8: Select the sketch and extrude it up to 5m.

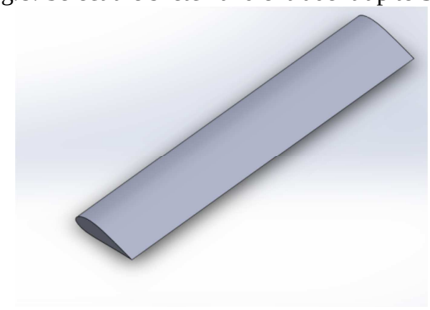

Fig.9: Final view of blade

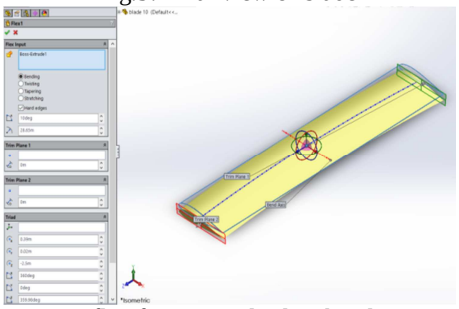

Fig.10: Go to flex feature, and select bend give 10 deg.

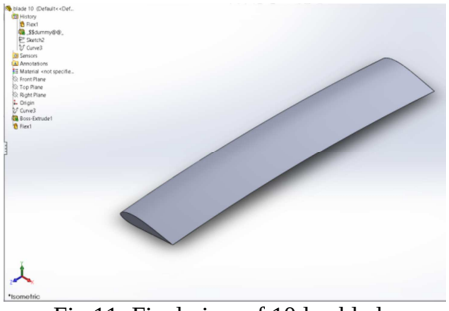

Fig.11: Final view of 10deg blade

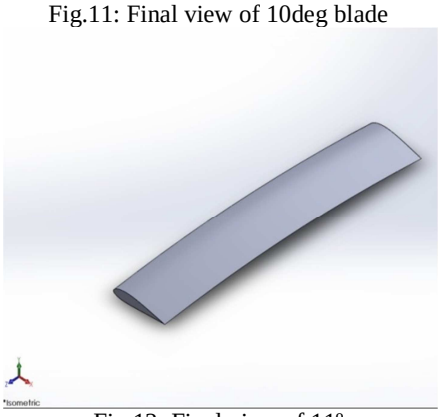

Fig.12: Final view of 11º

**FLOW ANALYSIS OF BLADE:**

***Materials Properties:***

| Materials | Density (Kg/m3) | Poison ratio | Young's modulus (Pa) |
|---|---|---|---|
| **E-glass** | 2000 | 0.3 | $50x10^{9}$ |
| **Carbon epoxy** | 1600 | 0.3 | $1.34x10^{11}$ |
| **Kevlar 29** | 1400 | 0.44 | 7.05E+10 |
| **Kevlar 49** | 1440 | 0.36 | 1.124E+11 |
| **Graphite epoxy** | 2260 | 0.25 | 151684.6604 |

Table.1: Materials properties

**FOR BLADE:**

Pressure contour

Velocity: 50 m/s

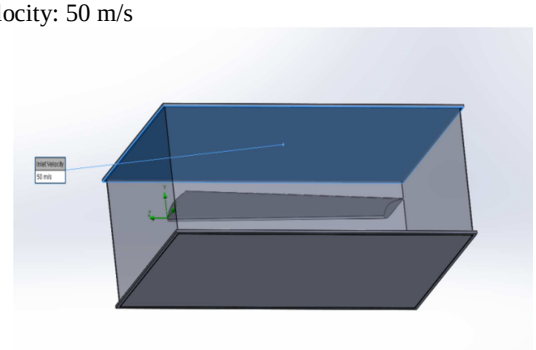

Fig.14: Applied velocity 50 m/s

Environmental pressure:

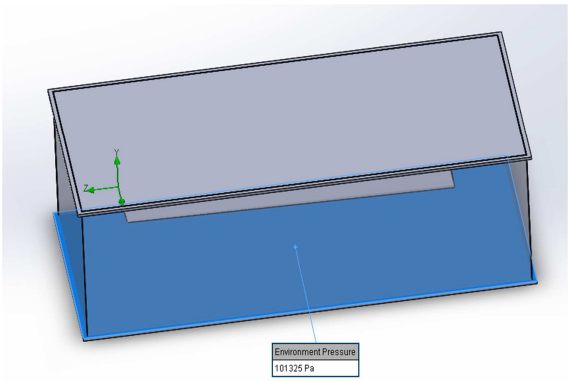

Fig.15: Applied environment pressure

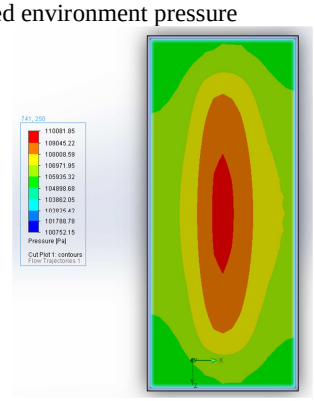

Fig.16: Pressure contour of blade
Velocity contour

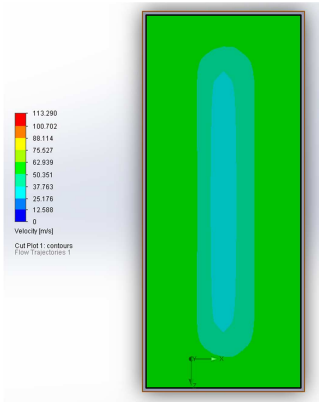

Fig.17: Velocity contour of blade Pressure flow

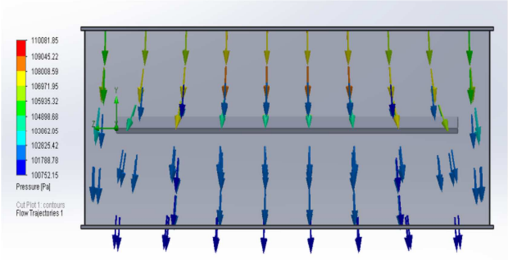

Fig.18: Pressure flow of blade Velocity flow

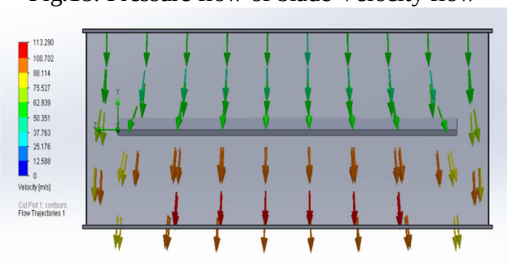

Fig.19: Velocity flow of blade

**FOR 10º:**
Pressure contour

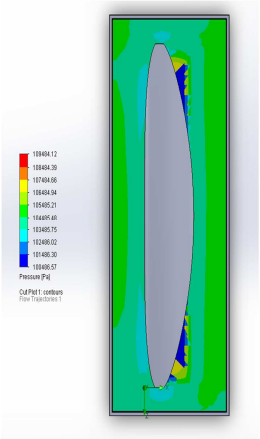

Fig.20: Pressure contour of blade of 10º
Velocity contour

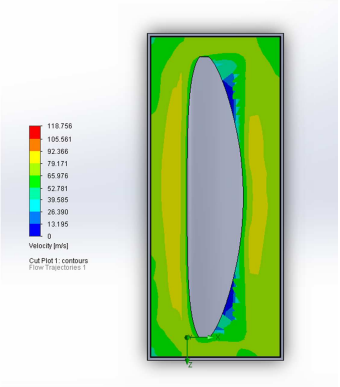

Fig.21: Velocity contour of blade of 10º
Pressure flow

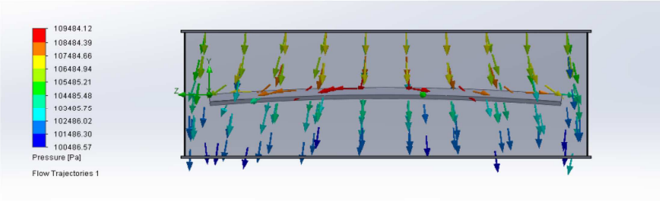

Fig.22: Pressure flow of blade 10º
Velocity flow

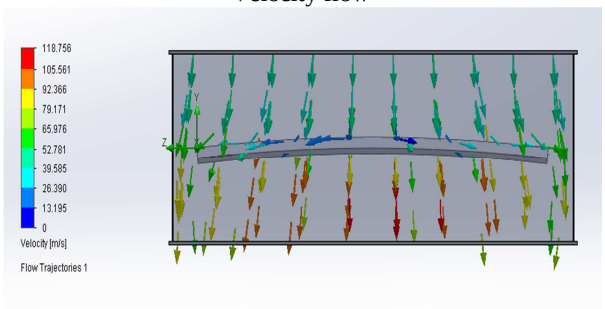

Fig.23: Velocity flow of blade 10º

**FOR 11º:**

Pressure contour

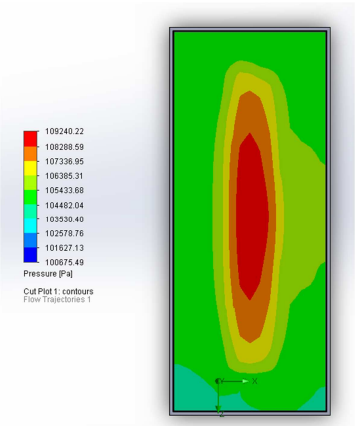


Fig.24: Pressure contour of blade of 11º

Velocity contour

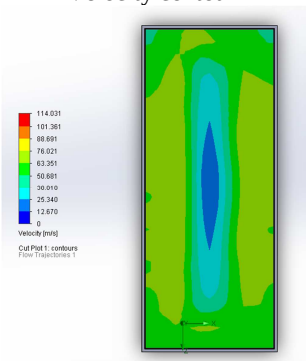


Fig.25: Velocity contour of blade 11º

Pressure flow

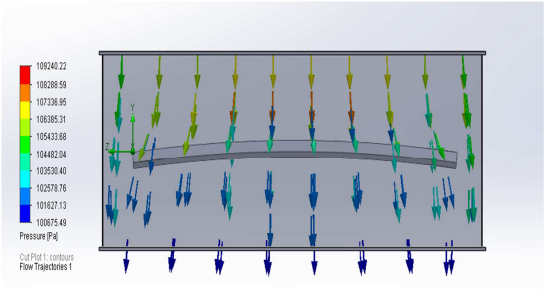


Fig.26: Pressure flow of blade 11º

Velocity flow

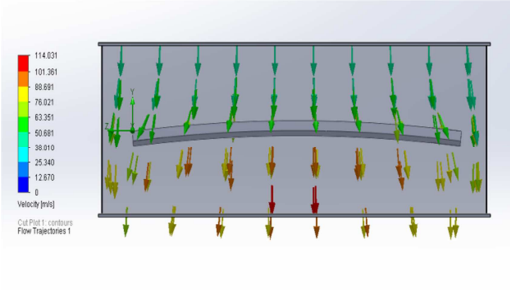


Fig.27: Velocity flow of blade 11º

**FOR 12º:**

Pressure contour

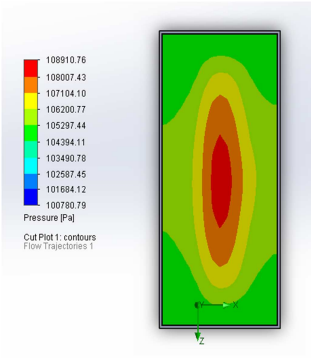


Fig.28: Pressure contour of blade of 12º

Velocity contour

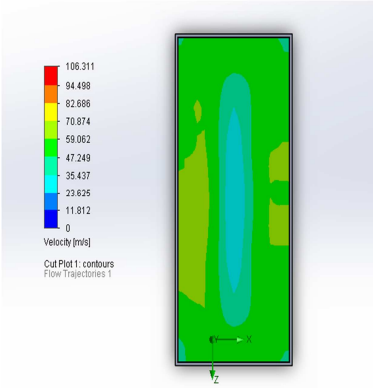


Fig.29: Velocity contour of blade of 12º

Pressure flow

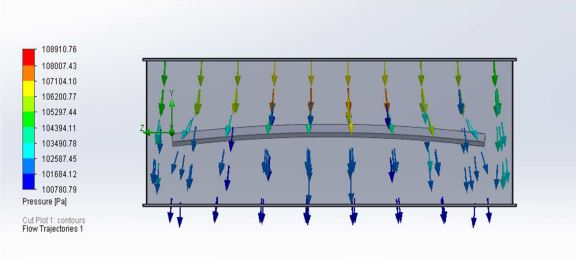


Fig.30: Pressure flow of blade 12º

Velocity flow

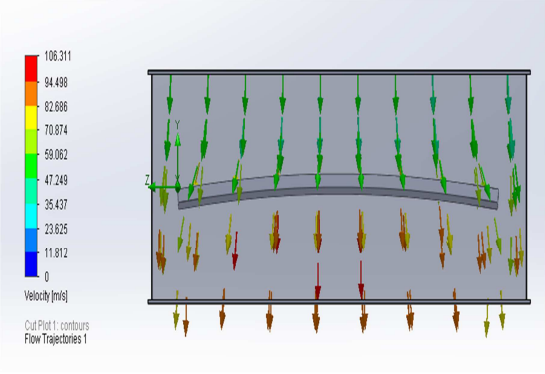


Fig.31: Velocity flow of blade 12º

## 5. INTRODUCTIONS TO ANSYS

ANSYS 16.0 delivers innovative, dramatic simulation technology advances in every major Physics discipline, along with improvements in computing speed and enhancements to enabling technologies such as geometry handling, meshing and post-processing..

ANALYSIS STEPS:

THE STEPS NEEDED TO PERFORM AN ANALYSIS DEPEND ON THE STUDY TYPE. YOU COMPLETE A STUDY BY PERFORMING THE FOLLOWING STEPS:

- Create a study defining its analysis type and options.
- If needed, define parameters of your study. A parameter can be a model dimension, material property, force value, or any other input.
- Define material properties.
- Specify restraints and loads.
- The program automatically creates a mixed mesh when different geometries (solid, shell, structural members etc.) exist in the model.
- Define component contact and contact sets.
- Mesh the model to divide the model into many small pieces called elements. Fatigue and optimization studies use the meshes in referenced studies.
- Run the study.
- View results

### *5.1. Static Analysis Of Blade:*

***For Blade***

Model

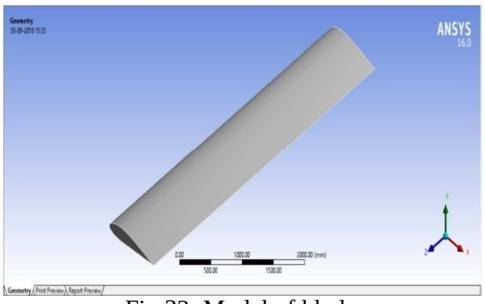


Fig.32: Model of blade

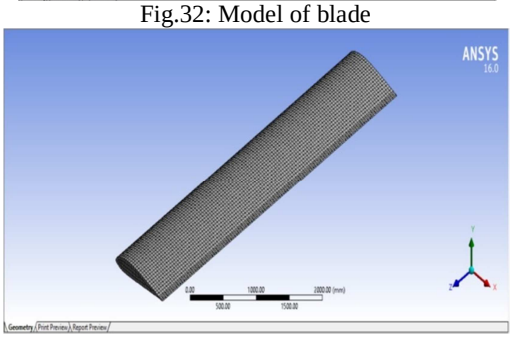


Fig.33: Mesh view of blade

Fixed support

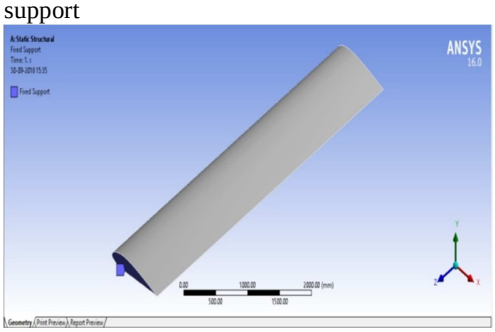


Fig.34: Fixed support of blade

Pressure: 1MPa

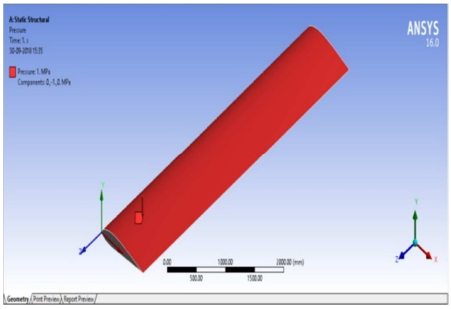


Fig.35: Pressure applied on the blade**E-glass epoxy**

Max. stress

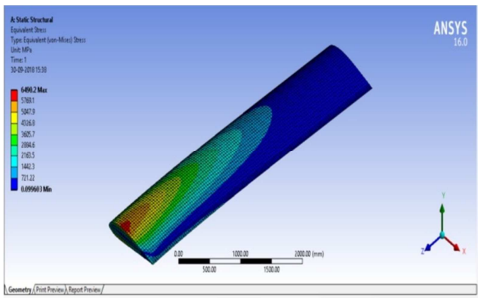


Fig.36: Maximum stress distribution of blade with E-glass epoxy material

Total deformation

Fig.37: Total deformation of blade with E-glass epoxy

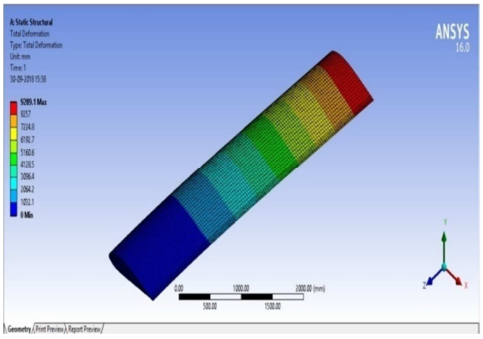


Max. strain

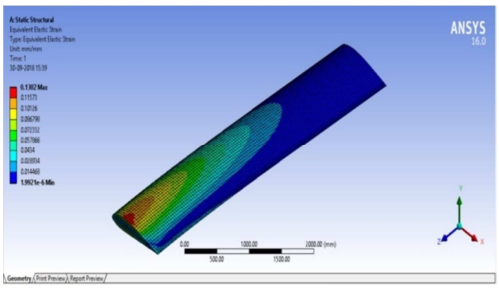


Fig.38: Maximum strain distribution of blade E-glass epoxy

**Carbon epoxy**

Max. stress

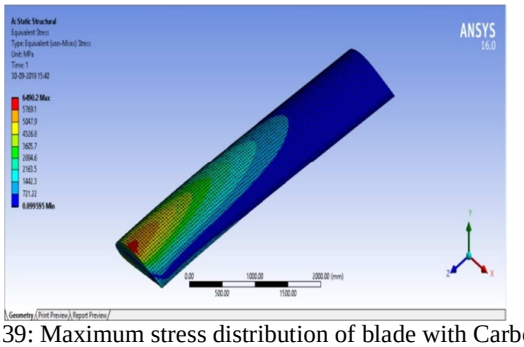


Fig.39: Maximum stress distribution of blade with Carbon epoxy material

Total deformation

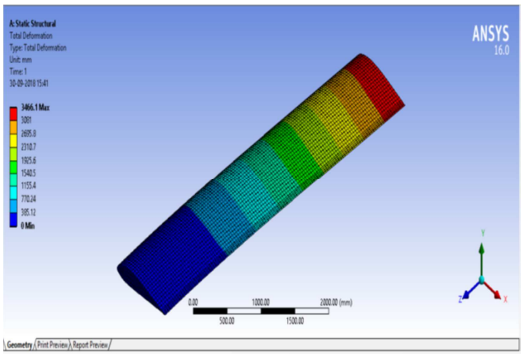


Fig.40: Total deformation of blade with Carbon epoxy material

Max. strain

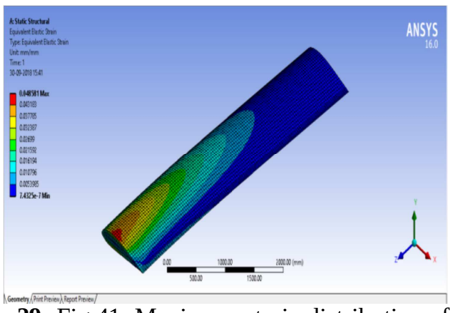


**Kevlar 29:** Fig.41: Maximum strain distribution of blade with Carbon epoxy material

Max. stress

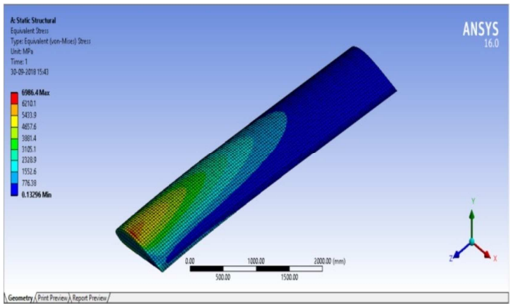


Fig.42: Maximum stress distribution of blade with Kevlar-29 material

Total deformation

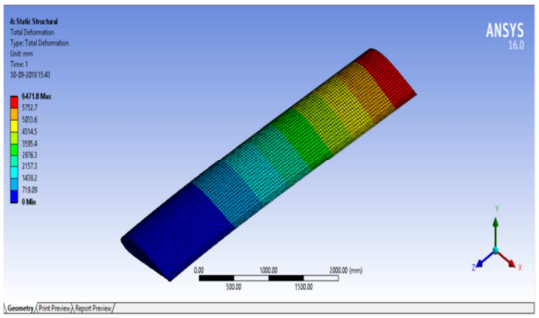


Fig.43: Total deformation of blade with Kevlar-29 material

Max. strain

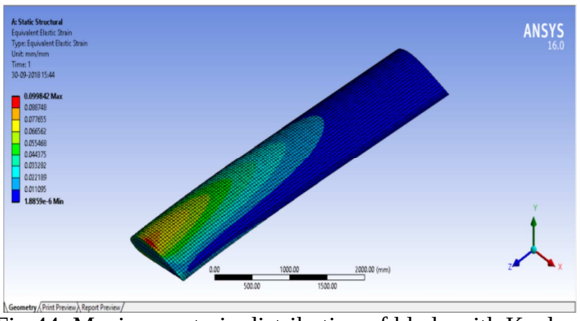


Fig.44: Maximum strain distribution of blade with Kevlar-29 material

**Kevlar 49:**

Max. stress

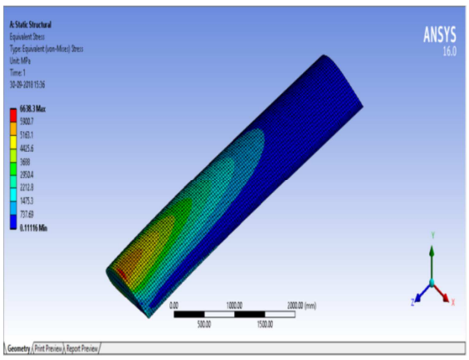


Fig.45: Maximum stress distribution of blade with Kevlar-49 material

Total deformation

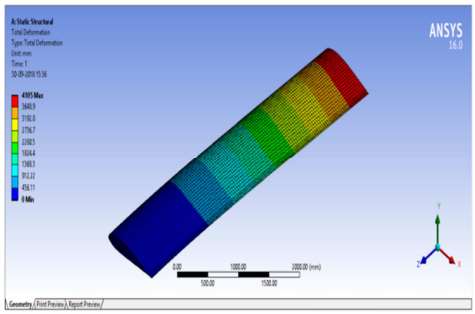


Fig.46: Total deformation of blade with Kevlar-49 material

Max. strain

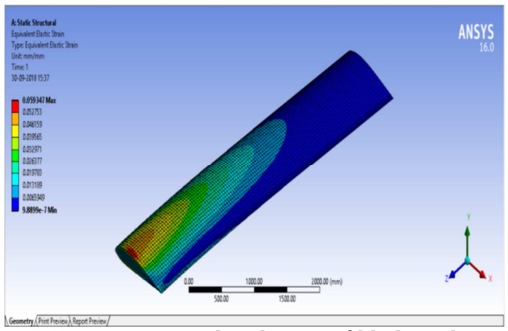


Fig.47: Maximum strain distribution of blade with Kevlar-49 material

**FOR 10º:**

Model

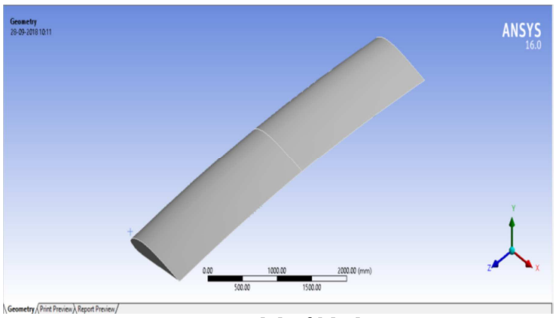


Fig.48: Model of blade 10º

Mesh

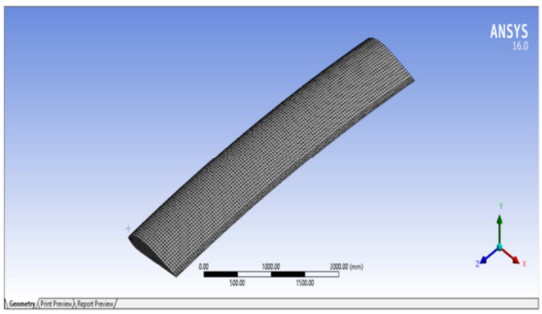


Fig.49: Mesh view of blade 10º

Fixed support

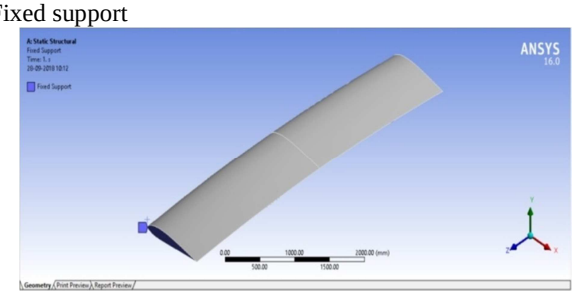


Fig.50: Fixed support of blade 10º

Pressure: 1MPa

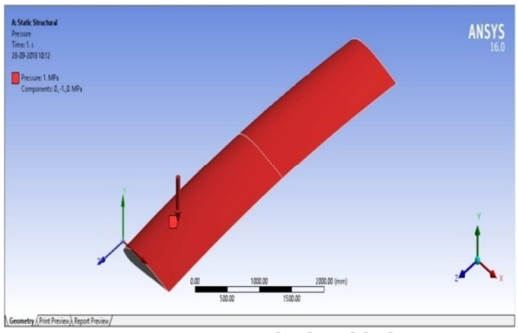


Fig.51: Pressure applied on blade 10º

**E-glass Epoxy:**

Max. stress

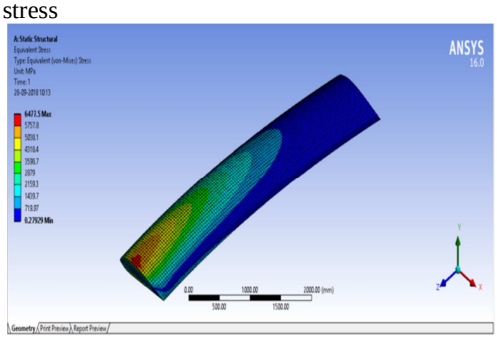


Fig.52: Maximum stress distribution of blade 10º with E-glass epoxy material

Total deformation

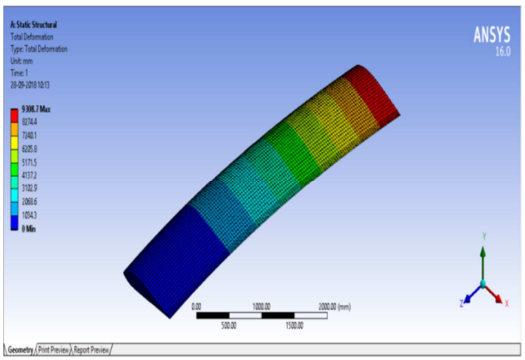

Fig.53: Total deformation of blade 10º with E-glass epoxy material

Max. strain

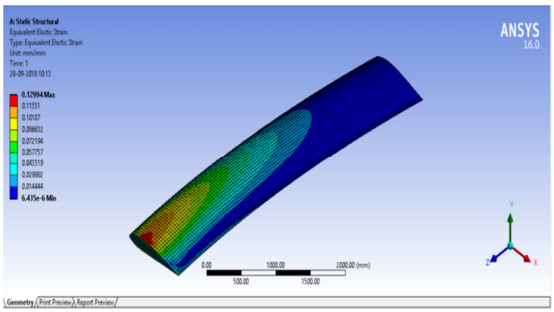

Fig.54: Maximum strain distribution of blade 10º with E-glass epoxy material

**Carbon epoxy:**

Max. stress

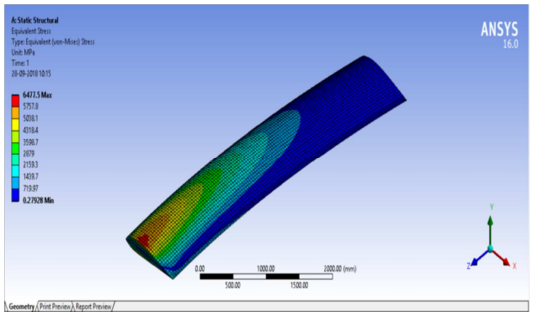

Fig.55: Maximum stress distribution of blade 10º with Carbon epoxy material

Total deformation

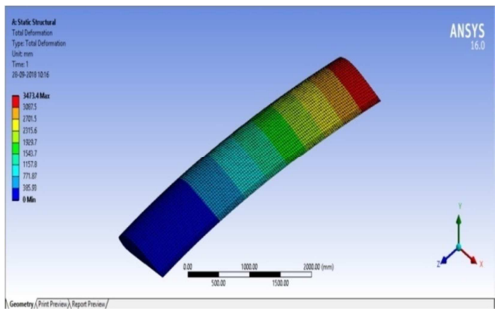

Fig.56: Total deformation of blade 10º with Carbon epoxy material

Max. strain

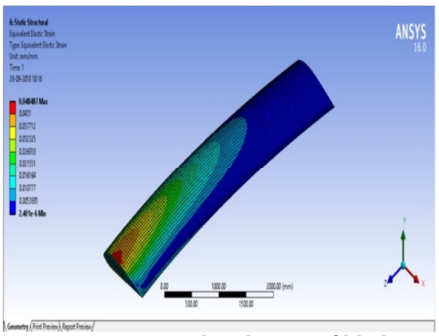

Fig.57: Maximum strain distribution of blade 10º with Carbon epoxy material

**Kevlar 29:**

Max. stress

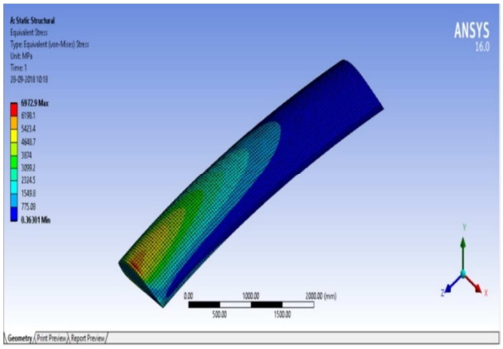

Fig.58: Maximum stress distribution of blade 10º with Kevlar-29 material

Total deformation

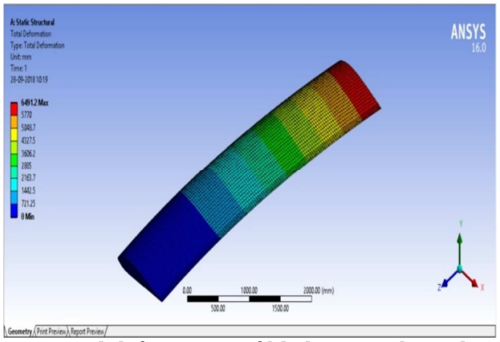

Fig.59: Total deformation of blade 10º with Kevlar-29 material

Max. strain

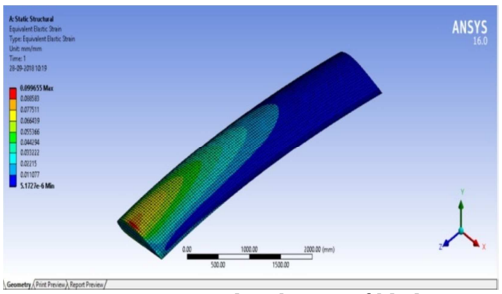

Fig.60: Maximum strain distribution of blade 10º with Kevlar-29 material

**Kevlar 49:**

Max. stress

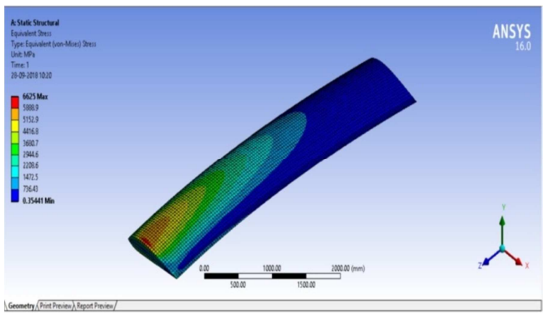


Fig.61: Maximum stress distribution of blade 10º with Kevlar-49 material

Total deformation

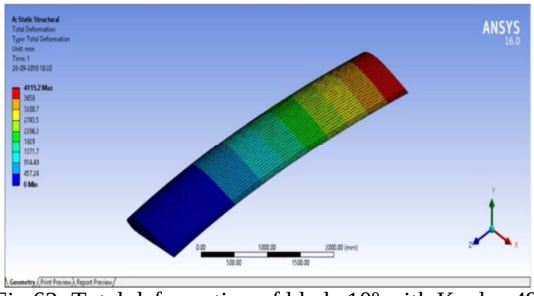


Fig.62: Total deformation of blade 10º with Kevlar-49 material

Max. strain

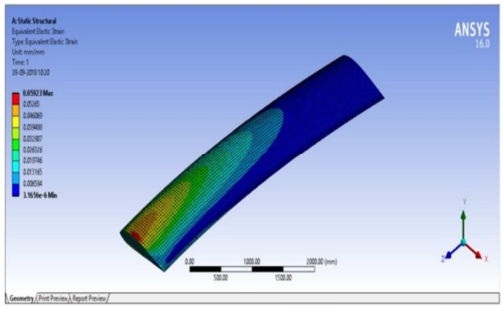


Fig.63: Maximum strain distribution of blade 10º with Kevlar-49 material

**FOR 11º:**

**E-glass epoxy:**

Max. stress

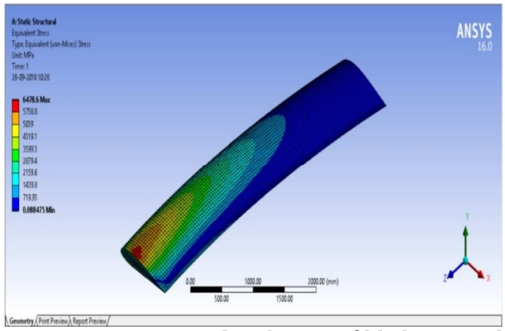


Fig.64: Maximum stress distribution of blade 11º with E-glass epoxy material

Total deformation

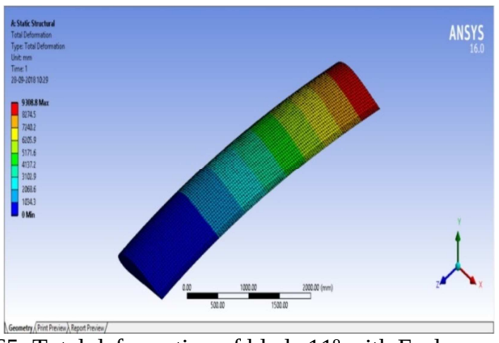


Fig.65: Total deformation of blade 11º with E-glass epoxy material

Max. strain

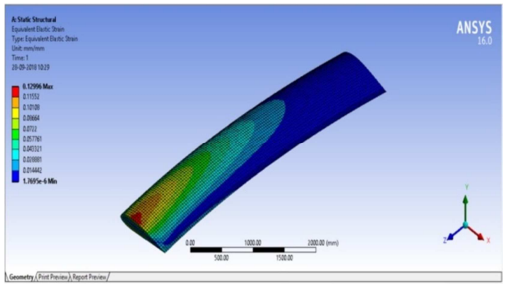


Fig.66: Maximum strain distribution of blade 11º with E-glass epoxy material

**Carbon epoxy:**

Max. stress

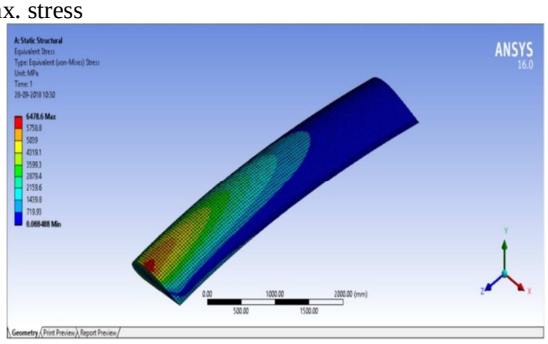


Fig.67: Maximum stress distribution of blade 11º with Carbon epoxy material

Total deformation

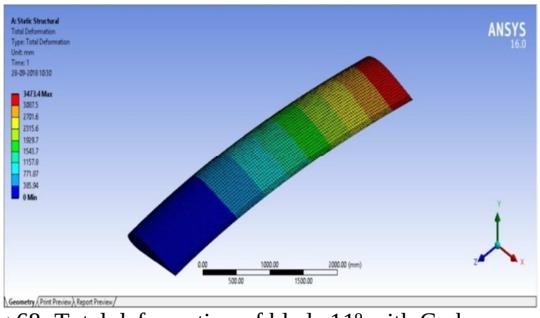


Fig.68: Total deformation of blade 11º with Carbon epoxy material

Max. strain

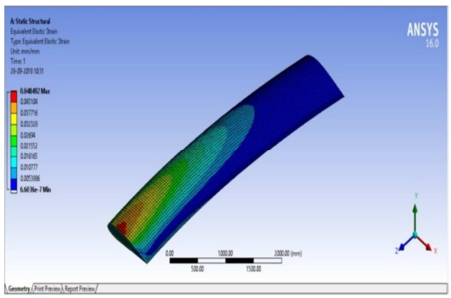


Fig.69: Maximum strain distribution of blade 11º with Carbon epoxy material

**Kevlar 29:**

Max. stress

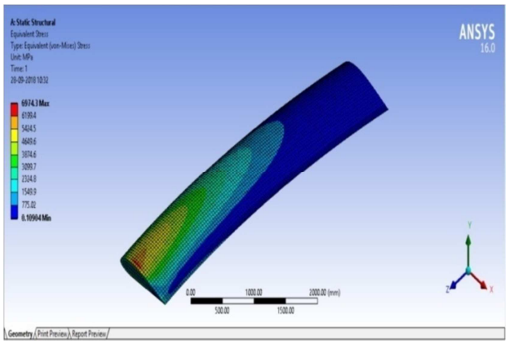


Fig.70: Maximum stress distribution of blade 11º with Kevlar-29 material

Total deformation

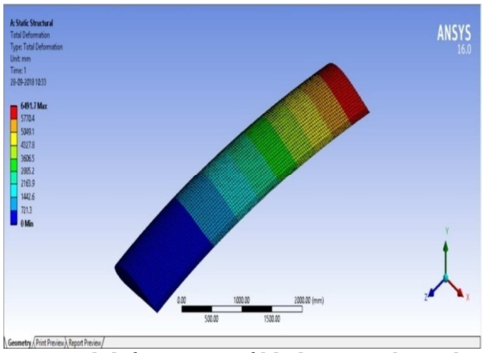


Fig.71: Total deformation of blade 11º with Kevlar-29 material

Max. strain

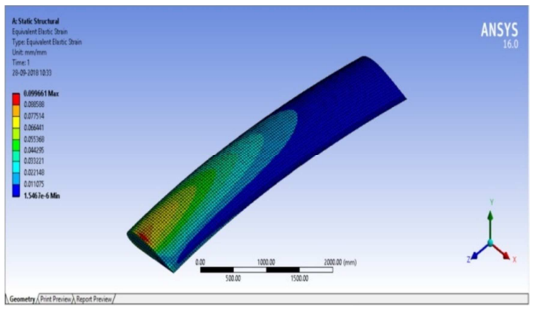


Fig.72: Maximum strain distribution of blade 11º with Kevlar-29 material

**Kevlar 49:**

Max. stress

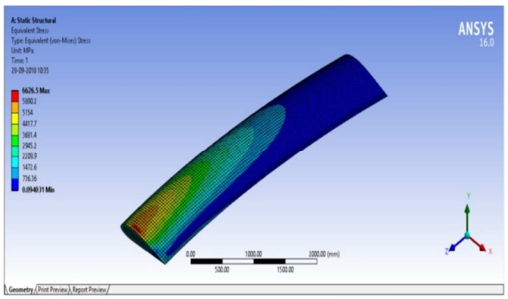


Fig.73: Maximum stress distribution of blade 11º with Kevlar-49 material

Total deformation

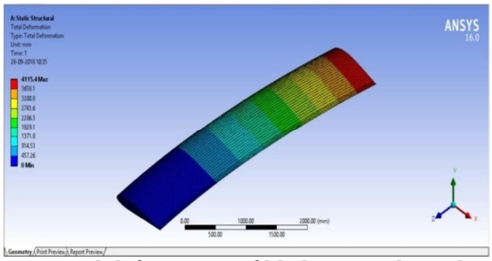


Fig.74: Total deformation of blade 11º with Kevlar-49 material

Max. strain

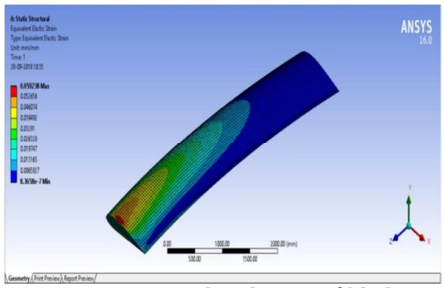


Fig.75: Maximum strain distribution of blade 11º with Kevlar-49 material

**FOR 12º:**

**E-glass epoxy**

Max. stress

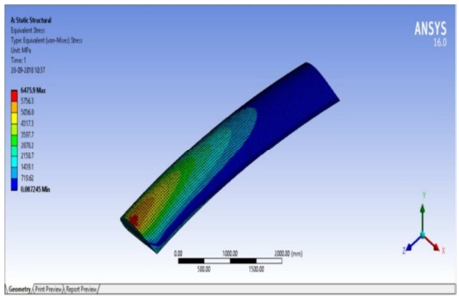


Fig.76: Maximum stress distribution of blade 12º with E-glass epoxy material

Total deformation

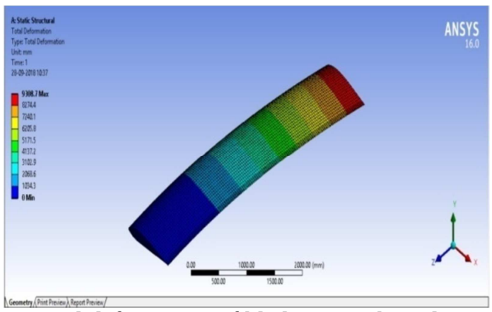


Fig.77: Total deformation of blade 12º with E-glass epoxy material

Max. strain

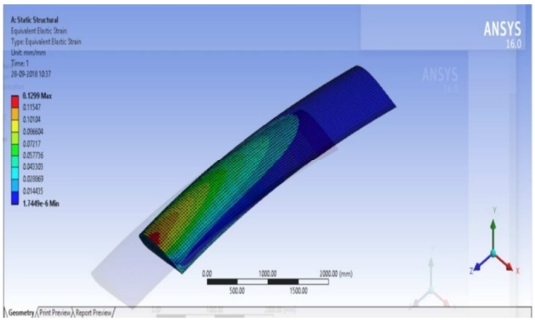


Fig.78: Maximum strain distribution of blade 12º with E-glass epoxy material

**Carbon epoxy:**

Max. stress

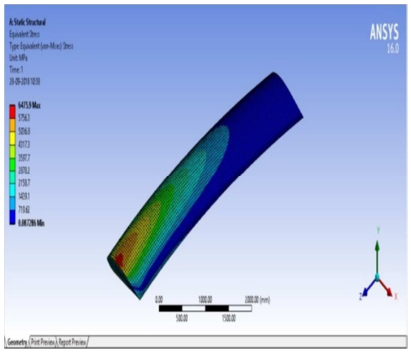


Fig.79: Maximum stress distribution of blade 12º with Carbon epoxy material

Total deformation

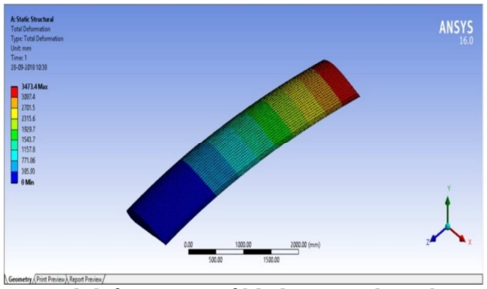


Fig.80: Total deformation of blade 12º with Carbon epoxy material

Max. strain

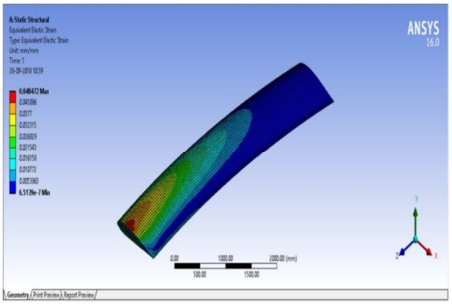


Fig.81: Maximum strain distribution of blade 12º with Carbon epoxy material

**Kevlar 29:**

Max. stress

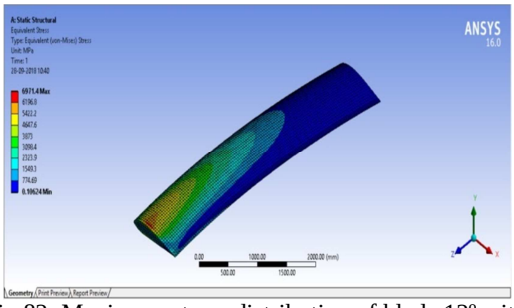


Fig.82: Maximum stress distribution of blade 12º with Kevlar-29 material

Total deformation

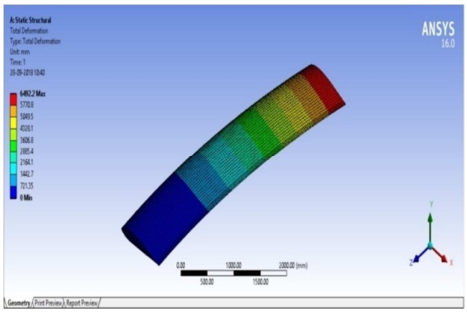


Fig.83: Total deformation of blade 12º with Kevlar-29 material

Max. strain

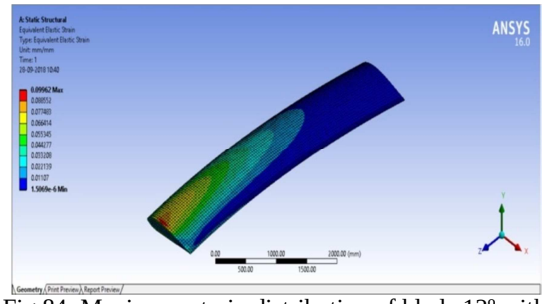


Fig.84: Maximum strain distribution of blade 12º with Kevlar-29 material

**Kevlar 49:**

Max. stress

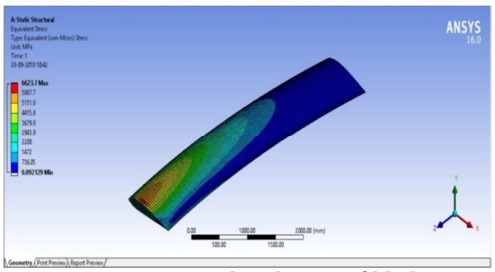


Fig.85: Maximum stress distribution of blade 12º with Kevlar-49 material

Total deformation

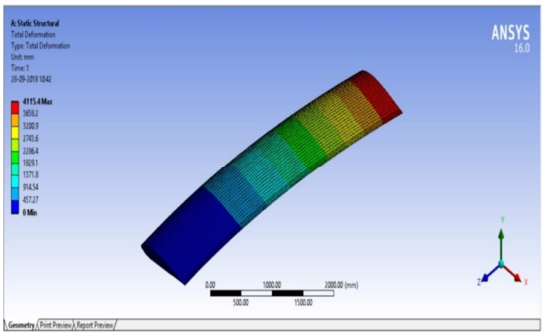


Fig.86: Total deformation of blade 12º with Kevlar-49 material

Max. strain

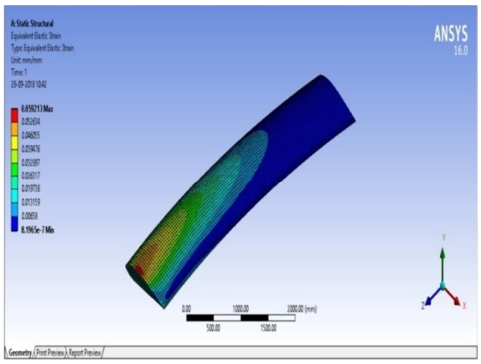


Fig.87: Maximum strain distribution of blade 12º with Kevlar-49 material

## 6. RESULTS:

*Static Analysis Results:*

For blade:

Table.2: Static results for blade

| Materials | Max. stress (MPa) | Total deformation (mm) | Max. strain |
|---|---|---|---|
| **E-glass** | 6490.2 | 9249.1 | 0.1302 |
| **Carbon fiber** | 64690.2 | 3466.1 | 0.048581 |
| **Kevlar 29** | 6986.4 | 6471.8 | 0.099842 |
| **Kevlar 49** | 6638.3 | 4105 | 0.059347 |

For 10º angle blade:

Table.3: Static results for 10º angle blade

| Materials | Max. stress (MPa) | Total deformation (mm) | Max. strain |
|---|---|---|---|
| **E-glass** | 6477.5 | 9308.7 | 0.12994 |
| **Carbon fiber** | 6477.5 | 3473.2 | 0.048487 |
| **Kevlar 29** | 6972.9 | 6491.2 | 0.099655 |
| **Kevlar 49** | 6625 | 4115.2 | 0.05923 |

For 11º angle blade:

Table.4: Static results for 11º angle blade

| Materials | Max. stress (MPa) | Total deformation (mm) | Max. strain |
|---|---|---|---|
| **E-glass** | 6478.6 | 9308.8 | 0.12996 |
| **Carbon fiber** | 6478.6 | 3473.4 | 0.048492 |
| **Kevlar 29** | 6974.3 | 6491.7 | 0.099661 |
| **Kevlar 49** | 6623.5 | 4115.4 | 0.059238 |

For 12º angle blade:

Table.5: Static results for 12º angle blade

| Materials | Max. stress (MPa) | Total deformation (mm) | Max. strain |
|---|---|---|---|
| **E-glass** | 6475.9 | 9308.7 | 0.1299 |

| | | | |
|---|---|---|---|
| **Carbon fiber** | 6475.9 | 3473.4 | 0.048472 |
| **Kevlar 29** | 6923.7 | 6492.2 | 0.09962 |
| **Kevlar 49** | 6623.7 | 4115.4 | 0.059213 |

*Flow Analysis Results***:**

Table.6: Flow analysis results

| Bend angle | Max. pressure (Pa) | Max. velocity (m/s) |
|---|---|---|
| **0** | 110081.85 | 113.290 |
| **10** | 109484.12 | 118.756 |
| **11** | 109240.22 | 114.031 |
| **12** | 108910 | 106.311 |

## 7. CONCLUSION:

In this project, static and flow simulation of wind turbine rotor blade for aero foil MH 102 type. In this, three types of designs by changing bend angles i.e. 10°, 11° and 12° and compared to original blade without angle.With different materials for static analysis i.e. E-glass epoxy, Carbon epoxy, Kevlar 29 and Kevlar 49.

The design completed in solid works 2014 and then converted into .igs form to import Ansys 16.0.In static analysis Apply pressure on the all blades is 1MPa and the optimum results shows that Carbon epoxy is the best.

In the flow analysis the air velocity 50 m/s given as boundary condition at environmental pressure and show the maximum pressure and velocity on 10°.As compared to previous (without angle) blade, with angle blade show the best results. Finally the 10° blade with Carbon epoxy is the best.

## 8. FUTURE SCOPE USEFULL FOR FORTHER STUDY:

The future scope of this project is to increase the efficiency of working of the blade. Another advantage is the deformations of the blade when change the bend angle is not much effect on the strength of blade.

We can use this this type of blades in the place of normal blades. The manufacture and maintenance is similar to the normal blades.

## REFERENCES

[1] Saxena G. and Agarwal M, 2013, "Aerodynamic analysis of NACA 4412 airfoil using CFD", International Journal of Emerging Trends in Engineering and Development,4, pp.416-423.

[2] McCosker J, 2012, “Design and optimization of a small wind turbine”, Rensselaer Polytechnic Institute Hartford, Connecticut, 3, pp.456-495.

[3] Oskarsdottir M, 2014, "A general description and comparison of horizontal axis wind turbines and vertical axis wind turbines", faculty of industrial engineering, mechanical engineering and computer science school of engineering and natural sciences university of Iceland reykjavik,

[4] Baldacchino D and van Bussel G, 2014, "Wind turbine wake stability investigations using a vortex ring modeling approach", Journal of Physics: Conference Series 555 012111.

[5] Sherry M, Sheridan J, Lo Jacono D, 2013, "Characterization of a horizontal axis wind turbine's tip and root vortices", Experiments Fluids 54, 1417.

[6] SerhatDuran S, 2012, “CAD design of horizontal axis wind turbine”, Renewable Energy, 44, pp. 252–260

[7] DeCoste et al., 2005, “Starting Torque Study of Darrieus Wind Turbine”- World Academy of Science, Engineering and Technology International Journal of Mathematical, Computational, Physical, Electrical and Computer Engineering Vol:9, 2015

[8] Herbert J. Sutherland and Paul S. Veers. 1995 “Effects of Cyclic Stress Distribution Models on Fatigue Life Predictions”, Wind Energy-, SED-Vol. 16, ASME, pp.83-90.

[9] Castillo, 2011, “Small Scale Vertical Axis Wind Turbine Design”- Bachelor’s Thesis, Tampere University of Applied Science.

[10] Deisadze et al., 2013, “Vertical Axis Wind turbine Evaluation and Design” Bachelor’s Thesis, Worcester Polytechnic Institute.

[11] G. ming, Y. Fei, Z. Jing, X. Yan-jun, 2010, “Design of Wind Turbine Blade based on Structure-First Approach” Information Engineering (ICIE), WASE International Conference, Vol 3, pp. 148-151

[12] Narimah et al., 2014, “Performance Evaluation of slotted and Continuous Types Wind Turbine Blades” Master’s Thesis, University Tun Hussein onn, Malaysia.

[13] Manyonge A W et al., 2012, “Mathematical ModelingOf Wind Turbine In a Wind Energy

Conversion System-Power Coefficient Analysis" Applied Mathematical Sciences, 6, pp. 4527-4533

[14] Griffiths, R T, 1977, the effect of airfoil characteristics on windmill performance. Aeronautical J. 81, pp.322– 326.

[15] Bottasso C L ET. 2014. Al "Structural Optimization of Wind Turbine Rotor Blades by Multi-Level Sectional/Multibody/3DFEM Analysis". MultibodySystemDynamics.Vol 32, pp 87-11

[16] Snel et al.,2003, "Review of Aerodynamics for Wind Turbines",Wind Energy Journal,vol 6, pp. 203-211

[17] Hassanein, A., El-Banna, H. & Abdel-Rahman, M. (2000) Effectiveness of airfoil aerodynamiccharacteristics on wind turbine designs performance. Proc. Seventh International Conference on Energy and Environment, vol. I. Cairo, Egypt, March 2000, 525– 537.